

Exploring the benefits of an asymmetric monostable potential function in broadband vibration energy harvesting

Aravind Kumar, Shaikh Faruque Ali, and A. Arockiarajan

Citation: *Appl. Phys. Lett.* **112**, 233901 (2018); doi: 10.1063/1.5037733

View online: <https://doi.org/10.1063/1.5037733>

View Table of Contents: <http://aip.scitation.org/toc/apl/112/23>

Published by the [American Institute of Physics](#)

Articles you may be interested in

[Sustaining high-energy orbits of bi-stable energy harvesters by attractor selection](#)

Applied Physics Letters **111**, 213901 (2017); 10.1063/1.5000500

[A double-stream Xe:He jet plasma emission in the vicinity of 6.7 nm](#)

Applied Physics Letters **112**, 221101 (2018); 10.1063/1.5016471

[Cadmium sulfide anchored in three-dimensional graphite cage for high performance supercapacitors](#)

Applied Physics Letters **112**, 223901 (2018); 10.1063/1.5025128

[Active magnetic force microscopy of Sr-ferrite magnet by stimulating magnetization under an AC magnetic field: Direct observation of reversible and irreversible magnetization processes](#)

Applied Physics Letters **112**, 223103 (2018); 10.1063/1.5030997

[High thermal conductivity and superior thermal stability of amorphous PMDA/ODA nanofiber](#)

Applied Physics Letters **112**, 221904 (2018); 10.1063/1.5031216

[Impurity dominated thin film growth](#)

Applied Physics Letters **112**, 221903 (2018); 10.1063/1.5021528

PHYSICS TODAY

WHITEPAPERS

MANAGER'S GUIDE

Accelerate R&D with
Multiphysics Simulation

READ NOW

PRESENTED BY

 COMSOL

Exploring the benefits of an asymmetric monostable potential function in broadband vibration energy harvesting

Aravind Kumar,^{a)} Shaikh Faruque Ali,^{b)} and A. Arockiarajan^{c)}

Department of Applied Mechanics, Indian Institute of Technology Madras, Chennai 600 036, India

(Received 27 April 2018; accepted 21 May 2018; published online 5 June 2018)

This letter explores the benefits offered by an asymmetric monostable potential function over the conventional symmetric linear and bistable potential functions in broadband vibration energy harvesting. Multi-stable harvesters such as the bistable and tristable harvesters provide an order of magnitude higher power than the linear harvesters while undergoing inter-well oscillations. However, when the excitation noise levels are insufficient to trigger inter-well oscillations, such harvesters provide very low power output. We propose a monostable configuration with an asymmetric potential energy function that is capable of providing a high energy output starting from excitation levels as low as $0.005 \text{ g}^2/\text{Hz}$ (g denotes acceleration due to gravity). The superior performance of the proposed asymmetric configuration over the conventional linear and bistable configurations is demonstrated through experiments, considering a band-limited white noise excitation. The experimental results also indicate that the asymmetric configuration delivers higher power at lower strain levels than the bistable configuration, mitigating the burden on the piezoelectric transducer. Thus, the asymmetric configuration offers a two-fold advantage in energy harvesting, leading to an increase in both the power output and the lifetime of the piezoelectric transducer.

Published by AIP Publishing. <https://doi.org/10.1063/1.5037733>

Energy harvesting has received great attention over the past decade as it could augment sustainable power supply to wireless sensor networks. Vibration energy harvesting is particularly attractive as mechanical vibrations are commonly available in industrial and structural environments and could act as a long term source of power for miniature devices monitoring such environments. The best performance of a conventional vibration energy harvester is usually limited to a harmonic excitation at its fundamental resonance frequency and at off-resonance frequencies, the power harvested is drastically reduced.^{1,2} To address this cardinal issue, a non-linear magneto-elastic interaction is often introduced to enhance the bandwidth of the system.^{3,4} Magneto-elastic structures with different types of potential energy function, such as monostable hardening,^{5–7} monostable softening,^{5,8} bistable,^{9–12} and tristable^{13–15} configurations have been explored extensively, to enable a high power output over a wide range of frequencies.

Recent efforts have been devoted to the evaluation of nonlinear harvesters under Gaussian white noise or colored noise excitation, which are more accurate representations of the ambient vibrations. Daqaq⁷ has provided a comprehensive analysis of the influence of stiffness nonlinearities on the power harvested from a piezoelectric energy harvester under a Gaussian white noise excitation. His results are in agreement with Cottone *et al.*¹⁶ who have shown that a bistable energy harvester provides a remarkable improvement over its linear counterpart only when the inter-well oscillations are activated. This requires either sufficiently large excitation to overcome the potential barrier^{17,18} or an appropriate impact mechanism to push the system to a high energy

orbit.¹⁹ Multi-stable harvesters, undergoing intra-well low energy oscillations, at very low excitation levels show no superiority over their linear counterparts.^{7,20} Hence, recent research focuses on developing harvesters with adaptive bistable potentials that significantly reduce the energy required to overcome the potential barrier. Both active²¹ and passive^{22,23} adaptive mechanisms have been explored to reduce the potential barrier and maximize the harvested energy. However, to ensure a complete relief from overcoming the potential barrier while retaining the benefits of nonlinear stiffness, a harvester with a nonlinear monostable potential could be used. A symmetric monostable hardening potential provides a substantial increase in the bandwidth under a harmonic or sweep excitation but it offers no benefit when compared with its linear counterpart under broadband random excitations.^{6,7} On the other hand, it has been shown through theoretical studies that, under a white noise excitation, monostable energy harvesting could benefit from asymmetries while the same is detrimental in bistable energy harvesting.²⁴ This brings about the interest to explore an asymmetric monostable potential as an alternative to a symmetric bistable potential, rather than using an asymmetric bistable or a symmetric monostable potential.

In this letter, we put forward the benefits offered by an asymmetric monostable potential in vibration energy harvesting over the symmetric bistable and linear potential functions. We show through experiments that the asymmetric monostable configuration can provide significant improvement in power output than the bistable and linear harvesters under a band-limited white noise excitation. Further, the asymmetric monostable configuration comes with an added advantage that the strain levels in the piezoelectric transducer are much lower than the bistable configuration, which translates to a longer lifetime of the piezoelectric transducer.

^{a)}Electronic mail: aravindkumarerode@gmail.com

^{b)}Electronic mail: sfali@iitm.ac.in

^{c)}Electronic mail: aarajan@iitm.ac.in

The proposed asymmetric monostable energy harvester consists of a cantilever beam with a magnet attached to its free end as illustrated in Fig. 1(a). A piezoelectric transducer is pasted in a unimorph configuration near the fixed end of the beam. A cylindrical bar magnet is placed below the vertical clamped position of the beam to introduce nonlinear magnetic interactions. The cylindrical magnet interacts in a repulsive manner with one of the poles of the tip magnet and attractive with another, resulting in an asymmetric monostable configuration. A conventional bistable harvester, on the other hand, consists of two external magnets, that always interact in an attractive manner with the pole of the tip magnet facing them as illustrated in Fig. 1(b). Due to this symmetry in interaction, the potential energy of the bistable harvester can be expressed as an even function with respect to the transverse tip displacement of the beam,²⁵

$$\Pi_b(w) = -b_1w^2 + b_2w^4, \quad (1)$$

where w denotes the dimensionless transverse displacement of the beam at its free end and b_1 and b_2 are system-dependent positive constants. Two stable static equilibrium positions occur at either side of the vertical clamped position of the beam at locations where the attractive magnetic force exactly cancels out the elastic restoring force in the beam as illustrated in Fig. 2. In the proposed monostable harvester, the asymmetric interaction between the base and the tip magnets results in,

$$\Pi_a(w) = -a_0 - a_1w - a_2w^2 + a_3w^3 + a_4w^4, \quad (2)$$

where the positive constants a_0 to a_4 depend on parameters such as modulus of elasticity of the beam and the magnet spacing and dimensions.²⁶ The lone static stable equilibrium position of the harvester occurs at the location where the repulsive magnetic force exactly cancels out the elastic restoring force in the beam, resulting in an asymmetric monostable configuration as illustrated in Fig. 2. Figure 2 shows the potential energy functions for the linear, bistable and asymmetric monostable configurations considered as, $\Pi_L = w^2$, $\Pi_B = w^4 - w^2$ and $\Pi_A = w^4 + 0.5w^3 - 0.25w^2 - 0.25w - 0.5$, respectively, for illustration.

The cantilever-type piezoelectric energy harvesters, shown in Fig. 1, are modeled as Euler-Bernoulli beams with

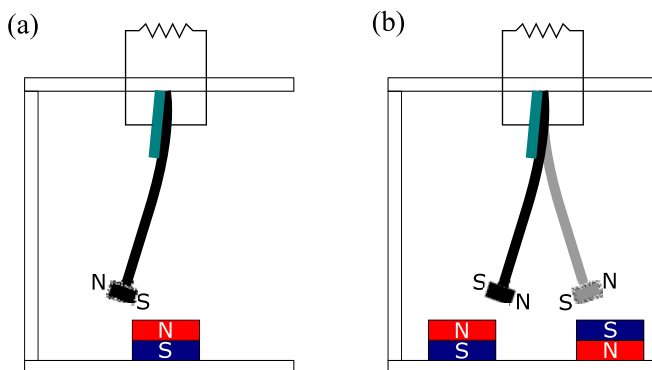


FIG. 1. Schematic representation of the piezomagnetoelastic energy harvester: (a) proposed asymmetric monostable configuration and (b) conventional bistable configuration.

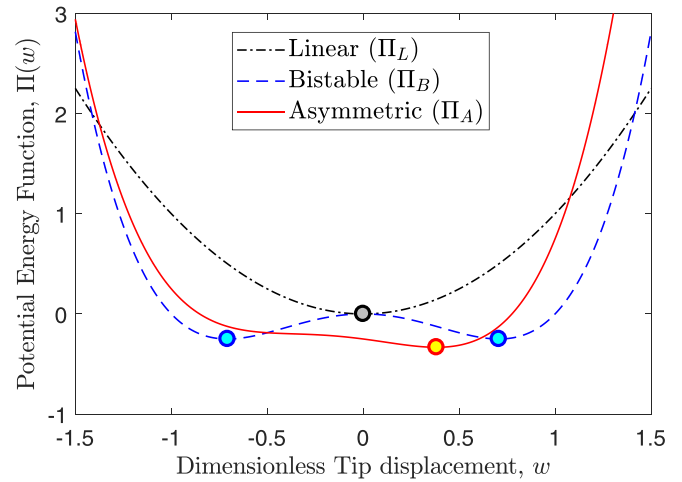


FIG. 2. Potential energy function of the different configurations considered for this study. The static stable equilibrium positions of each configuration are indicated using circle markers of the associated color.

appropriate boundary conditions.²⁷ The fundamental mode dominates the response of the system for the excitation bandwidth considered. Hence, for a single mode approximation, the equations of motion of the harvester are expressed in a non-dimensional form as follows,

$$\ddot{w} + 2\zeta\omega_n\dot{w} + \frac{d\Pi}{dw} - \chi v = f(t), \quad (3)$$

$$\dot{v} + \lambda v - \kappa\dot{w} = 0, \quad (4)$$

where v is the dimensionless voltage, ζ is the damping ratio, ω_n is the dimensionless linearized natural frequency, and λ is the decay constant of the electrical circuit. The terms χ and κ represent the dimensionless electromechanical coupling coefficients. The restoring force in the system is the derivative of the potential energy function, $h(w) = \frac{d\Pi}{dw}$. The excitation $f(t)$ is proportional to the base acceleration.

Three different configurations of the harvester, namely, linear, bistable and asymmetric monostable configurations were considered for experiments and tested under a band-limited white noise excitation. Figure 3 shows the experimental prototype of the proposed energy harvester as a cantilever beam of dimensions 90 mm × 10 mm × 0.26 mm, made of spring steel. A Macro Fiber Composite transducer of model M2807-P2, manufactured by Smart Material Corp. is pasted in a unimorph configuration near the fixed end of the beam. Two small cylindrical Neodymium magnets, each of length 5.95 mm, diameter 4.97 mm and mass 6.1 g are attached on either side of the free end of the beam. For the proposed asymmetric configuration, a rare earth magnet of diameter 24.81 mm and thickness 2.92 mm is placed below the vertical clamped position of the beam. For the bistable configuration, two Neodymium magnets of diameter 24.92 mm and thickness 3.01 mm are placed symmetrically on either side of the vertical clamped position of the beam. The entire setup is mounted to a slip table which is excited by an electro-dynamic shaker MPA101-L215M of make “ETS solutions.” The operation of the shaker is regulated with the help of a feedback based VR Medallion controller. The tip displacement of the beam is measured with the help

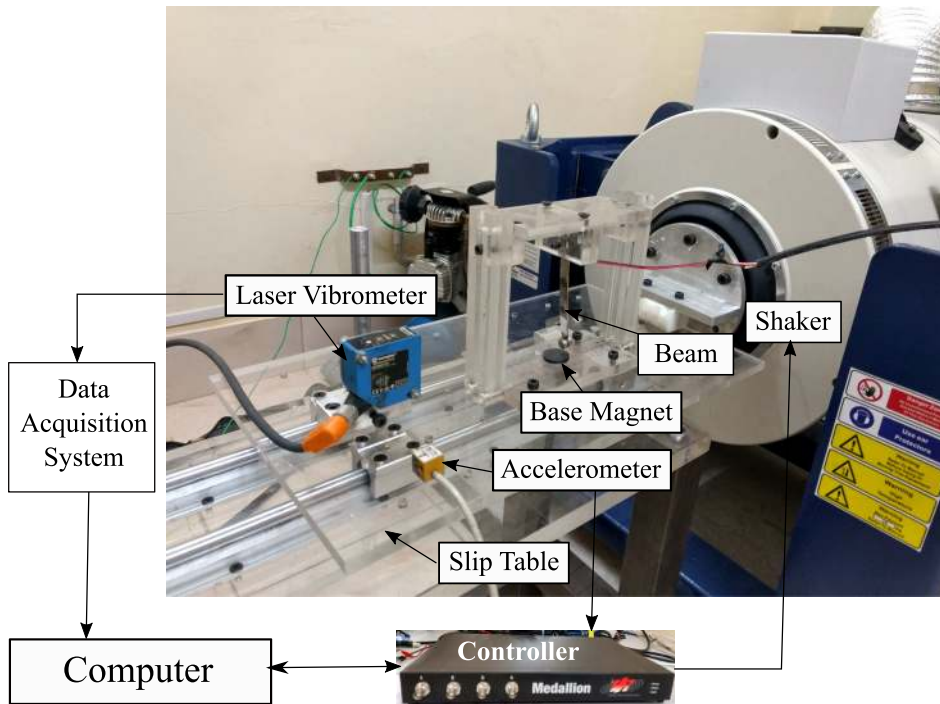


FIG. 3. Experimental test rig, showing the asymmetric energy harvester mounted on a slip table.

of a laser vibrometer. Data acquisition is enabled using NI DAQ integrated with LabView[®] software. The average power harvested from the system is calculated as, $P = \frac{E|V|^2}{R_l}$. Here, R_l represents the load resistance and V represents the potential difference across that load resistance. The excitation bandwidth was fixed at 10–30 Hz while five different values of load resistance were deployed for the analysis.

The experimentally obtained phase portraits and voltage time histories for the asymmetric monostable and the bistable configurations, for a load resistance of 6.7 k Ω , are shown in Fig. 4. The average power harvested is also indicated therein. The phase portrait of the asymmetric energy harvester, illustrated in Fig. 4(a), consists of two distinctive lobes which arise due to the asymmetry of the potential energy function. As observed from Fig. 4, the asymmetric harvester exhibits a response with comparatively larger amplitudes of displacement and voltage at a very low excitation level of 0.005 g²/Hz (g denotes acceleration due to gravity) while the bistable harvester exhibits low amplitude intra-well oscillations at such excitation levels. Consequently, at 0.005 g²/Hz, the power output of the asymmetric configuration ($P = 15.432 \mu\text{W}$) is around 20 times higher than that of the bistable configuration ($P = 0.749 \mu\text{W}$), as indicated in Fig. 4. The bistable harvester

produces a comparable power output ($P = 16.812 \mu\text{W}$) only at 0.02 g²/Hz, while it undergoes inter-well oscillations. The intra-well and inter-well responses of the bistable harvester are shown in Figs. 4(b) and 4(c), respectively.

The performance of different configurations under increasing excitation levels has been tested by varying the excitation amplitude from 0.005 g²/Hz to 0.025 g²/Hz in steps of 0.005 g²/Hz. The power harvested from different configurations is plotted against the excitation amplitude for two different load resistances in Fig. 5. It is evident from Fig. 5 that both the bistable and the proposed asymmetric monostable configurations provide a power output several magnitudes higher than that of the linear configuration. Among the two nonlinear configurations, the asymmetric configuration provides a better power output than the bistable configuration. The difference between the two configurations is prominent for lower levels of excitation due to the absence of a potential barrier in the proposed asymmetric configuration.

Further, the performance of different configurations has been explored under varying load resistances and the corresponding results are shown in Fig. 6. Five different values of load resistance, 0.98 k Ω , 6.7 k Ω , 11.85 k Ω , 65 k Ω , and 133 k Ω have been used for the analysis. It could be seen that

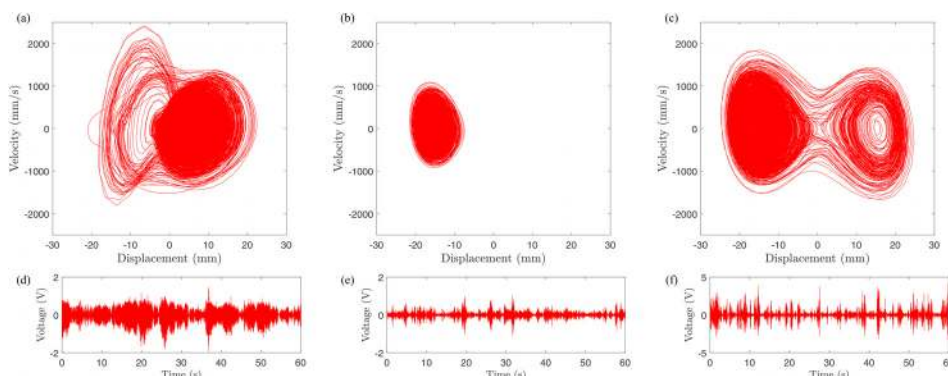


FIG. 4. Experimental phase portraits and voltage time histories corresponding to: (a) and (d) asymmetric harvester at an excitation level of 0.005 g²/Hz ($P = 15.432 \mu\text{W}$), (b) and (e) intra-well response of the bistable harvester at 0.005 g²/Hz ($P = 0.749 \mu\text{W}$), and (c) and (f) inter-well response of the bistable harvester at 0.02 g²/Hz ($P = 16.812 \mu\text{W}$).

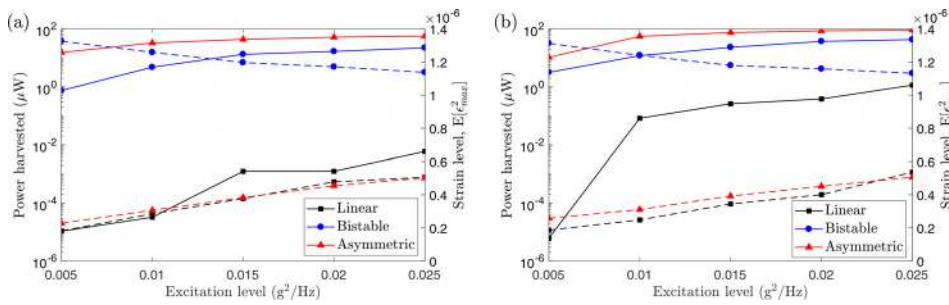


FIG. 5. Variation in the power harvested (represented as solid lines) and the strain level (represented as dashed lines) for different configurations with respect to the excitation amplitude for load resistances of (a) 6.7 kΩ and (b) 11.85 kΩ.

the asymmetric monostable harvester consistently outperforms the bistable and the linear harvesters for various values of the load resistances considered. Further, the power harvested from all the three different configurations is maximum at a load resistance of 11.85 kΩ among the various values of resistances considered.

Yet another crucial, but generally overlooked aspect in energy harvesting is the life expectancy of the harvester. The lifetime of the piezoelectric transducer reduces with increase in the strain it is subjected to.^{28,29} The strain in the piezoelectric transducer can be calculated from the tip displacement of the harvester by assuming a suitable deformation profile for the beam. We assume,²⁶

$$\phi(x) = 1 - \cos\left(\frac{\pi x}{2L}\right), \quad (5)$$

where L is the length of the beam. Hence, the displacement at any point in the beam can be related to the tip displacement as follows,

$$w_p(x, t) = w(t) \left(1 - \cos\left(\frac{\pi x}{2L}\right)\right). \quad (6)$$

Strain at any point in the beam can be calculated as,

$$\epsilon_x(z, x, t) = z \frac{\partial^2 w_p}{\partial x^2} = z w(t) \frac{\pi^2}{4L^2} \cos\left(\frac{\pi x}{2L}\right), \quad (7)$$

where z represents the distance from the neutral axis of the beam.

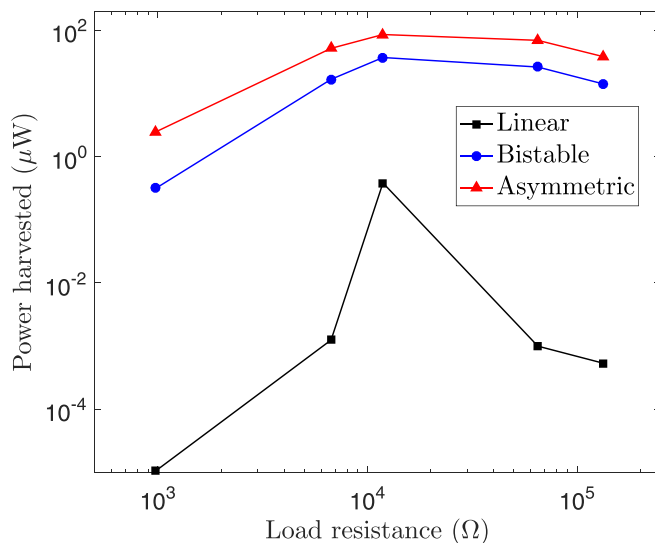


FIG. 6. Variation in the power harvested for different configurations with respect to the load resistance at an excitation level of 0.02 g²/Hz.

In a unimorph cantilever type piezoelectric energy harvester, the maximum strain in the piezoelectric transducer occurs at the outermost fiber at the fixed end of the beam. Hence, substituting $x=0$ and $z = \frac{E_b A_b (t_p + t_b)}{2(E_b A_b + E_p A_p)}$ in Eq. (7), we get,

$$\epsilon_{max}(t) = \frac{\pi^2 E_b A_b (t_p + t_b)}{8L^2 (E_b A_b + E_p A_p)} w(t). \quad (8)$$

As the base excitation provided to the beam, $f(t)$ is a random process, the tip displacement of the beam $w(t)$ and consequently, the maximum strain in the piezoelectric transducer $\epsilon_{max}(t)$ are also random processes. Hence, we use the second raw moment of the maximum strain, $E[\epsilon_{max}^2]$ as a measure to quantitatively compare the maximum strain levels among the different configurations of the harvester, which is given as,

$$E[\epsilon_{max}^2] = \left(\frac{\pi^2 E_b A_b (t_p + t_b)}{8L^2 (E_b A_b + E_p A_p)}\right)^2 E[w^2]. \quad (9)$$

The bistable configuration (when undergoing intra-well oscillations) and the asymmetric configuration generally have a non-zero mean displacement response. The use of a central moment would ignore the effect of the strain resulting from this non-zero mean displacement. Instead, the second raw moment is used to accurately capture the strain levels undergone by the transducer.

In Fig. 5, the strain levels ($E[\epsilon_{max}^2]$) for the linear, bistable and the asymmetric monostable configurations are also displayed alongside the power harvested. For similar levels of excitation, the asymmetric monostable configuration undergoes strain levels that are comparable to that of the linear configuration while the strain levels in the bistable configuration are twice than that of the former. Thus, the proposed asymmetric configuration combines the advantages of both the linear and the bistable configurations by providing a high power output while exhibiting lower strain levels. The lower strain levels mitigate the fatigue damage taken by the piezoelectric transducer and prolong the life of the harvester.²⁹

In summary, this letter explores the benefits offered by an asymmetric monostable potential function in piezoelectric energy harvesting under low amplitude broadband excitations. The key advantages of the proposed configuration are two-fold. First, the asymmetric monostable potential function offsets the need for overcoming a potential barrier that generally appears in a bistable configuration, providing a better power output for very low levels of excitation. Second, it is observed from the experiments that for the same level of excitation, the asymmetric configuration undergoes significantly lower strain

levels while providing a higher power output when compared to the bistable configuration. This is extremely beneficial from a material standpoint as a lower strain level translates to a higher lifetime of the harvester. Thus, the notion of asymmetric mono-stability discussed here is highly suitable for piezoelectric energy harvesting and can be further extended to electromagnetic and electrostatic harvesters based on magneto-elastic structures.

The authors are thankful to the Department of Science and Technology, India, for funding the research work (Project No. DST-YSS/2014/000336).

- ¹L. Gammaitoni, I. Neri, and H. Vocca, *Appl. Phys. Lett.* **94**, 164102 (2009).
- ²D. D. Quinn, A. L. Triplett, L. A. Bergman, and A. F. Vakakis, *J. Vib. Acoust.* **133**, 011001 (2011).
- ³R. Ramalan, M. J. Brennan, B. R. Mace, and I. Kovacic, *Nonlinear Dyn.* **59**, 545 (2010).
- ⁴M. F. Daqaq, R. Masana, A. Erturk, and D. Quinn, *Appl. Mech. Rev.* **66**, 040801 (2014).
- ⁵S. C. Stanton, C. C. McGehee, and B. P. Mann, *Appl. Phys. Lett.* **95**, 174103 (2009).
- ⁶D. A. W. Barton, S. G. Burrow, and L. R. Clare, *J. Vib. Acoust.* **132**, 021009 (2010).
- ⁷M. F. Daqaq, *Nonlinear Dyn.* **69**, 1063 (2012).
- ⁸K. Fan, Q. Tan, Y. Zhang, S. Liu, M. Cai, and Y. Zhu, *Appl. Phys. Lett.* **112**, 123901 (2018).
- ⁹A. Erturk, J. Hoffmann, and D. J. Inman, *Appl. Phys. Lett.* **94**, 254102 (2009).
- ¹⁰S. C. Stanton, C. C. McGehee, and B. P. Mann, *Phys. D* **239**, 640 (2010).
- ¹¹B. P. Mann and B. A. Owens, *J. Sound Vib.* **329**, 1215 (2010).
- ¹²A. Erturk and D. J. Inman, *J. Sound Vib.* **330**, 2339 (2011).
- ¹³S. Zhou, J. Cao, D. J. Inman, J. Lin, S. Liu, and Z. Wang, *Appl. Energy* **133**, 33 (2014).
- ¹⁴S. Zhou, J. Cao, D. J. Inman, S. Liu, W. Wang, and J. Lin, *Appl. Phys. Lett.* **106**, 093901 (2015).
- ¹⁵P. Kim, D. Son, and J. Seok, *Appl. Phys. Lett.* **108**, 243902 (2016).
- ¹⁶F. Cottone, H. Vocca, and L. Gammaitoni, *Phys. Rev. Lett.* **102**, 080601 (2009).
- ¹⁷G. Litak, M. I. Friswell, and S. Adhikari, *Appl. Phys. Lett.* **96**, 214103 (2010).
- ¹⁸S. F. Ali, S. Adhikari, M. I. Friswell, and S. Narayanan, *J. Appl. Phys.* **109**, 074904 (2011).
- ¹⁹J. Cao, S. Zhou, W. Wang, and J. Lin, *Appl. Phys. Lett.* **106**, 173903 (2015).
- ²⁰A. Erturk and S. Zhao, *Appl. Phys. Lett.* **102**, 103902 (2013).
- ²¹A. H. Hosseinloo and K. Turitsyn, *Smart Mater. Struct.* **25**, 015010 (2016).
- ²²A. H. Hosseinloo and K. Turitsyn, *Phys. Rev. Appl.* **4**, 064009 (2015).
- ²³G. Shan, D. F. Wang, J. Song, Y. Fu, and X. Yang, "A spring-assisted adaptive bistable energy harvester for high output in low-excitation," *Microsyst. Technol.* (published online 2018).
- ²⁴Q. He and M. F. Daqaq, *J. Sound Vib.* **333**, 3479 (2014).
- ²⁵F. C. Moon and P. J. Holmes, *J. Sound Vib.* **65**, 275 (1979).
- ²⁶K. A. Kumar, S. F. Ali, and A. Arockiarajan, *J. Sound Vib.* **393**, 265 (2017).
- ²⁷A. Erturk and D. J. Inman, *Smart Mater. Struct.* **18**, 025009 (2009).
- ²⁸P. V. Avvari, Y. Yang, and C. K. Soh, *J. Intell. Mater. Syst. Struct.* **28**, 1188 (2017).
- ²⁹A. Pandey and A. Arockiarajan, *Compos. Struct.* **174**, 301 (2017).